13 Gels

13.1 Structure of Gels

In general, a disperse system which can behave like a soft solid, without appreciably changing the neighboring topology under an external stress, is called a gel. It easily deforms under shear, but is quite incompressible under hydrostatic pressure. There are in nature many examples of gels. Biological systems mainly consist of gels. Gels have surprisingly wide practical applications. On the other hand, systems which have a good fluidity like a liquid are named as sols.

Colloidal particles in sols are very often solvated to a thickness of about one molecul. Much greater amounts of solvent can be sometimes entrapped within particle aggregates or flocculent precipitates. In solutions, the polymer chains may cross-link and become mechanically entangled to such an extent that a continuous network is formed. If all of the solvent is trapped within this network, the system as a whole takes on a solid appearance and is a gel.

Jellies are considered as one type of gel and have similar structures. In these, the units of the aggregates are primarily spherical or linear, but these are sufficiently linked so that the whole liquid is enmeshed into a loose three-dimensional framework. Thus, in gels or jellies both the solid and liquid components are in a highly dispersed state.

Some of the entrapped water or ions behave in nearly the same way as in bulk water (Alexander and Johnson, 1949, p. 602). The electrophoretic mobility of H_3O^+ was reported in 1886 to be 25 μm/s per volt per cm in an ingenious experiment. In this experiment a tube of gelled alkaline solution containing phenolphthalein indicator was dipped in acid as the rate of movement of the boundary between colorless and pink gel was measured in an applied field. The bulk value was reported as 32 μm/s per volt per cm. Brown and Chitumbo (1975) carefully measured the diffusion coefficients of water, various alcohols, and solutions of LiCl, NaCl, KCl, etc. in aqueous cellulose gels at 25°C. The observed result indicates that the diffusion coefficients of solvents and solutes in the gels are 17 to 27% of the bulk values. The reduction in the values is considered to be due to an increase of the effective viscosity of water in the gels, possibly due to interactions with cellulose. The effect of molecular size is small. The freezing point of some water in a gelatin gel or polyvinyl alcohol gel is lowered to below –196°C due to interactions with the gel (Higuchi and Iijima, 1985). Water molecules near the gel

framework are highly oriented (within one-molecular thickness) and the rotational relaxation time is 10^{-5} to 10^{-6} s, compared to the balk value of 10^{-12} s. The amount of water falling to this class differs from gel to gel. Such behavior of water is observed in biological cells, where about 10% of water is strongly interacting with polymers and the freezing point is very low. About 80% of water in the cells has the rotational relaxation time of about 10^{-8} to 10^{-9} s and the freezing point at –10°C to –20°C. The spin-spin relaxation time of water has been also observed to have different peaks in gels and sols (Tokita et al., 1990).

In order to form a three-dimensional structure, at least some particles must be joined to three or more others due to van der Waals' interactions, electrostatic forces, hydrogen bonding, or chemical reactions. Heat-reversible gels have junction points that are loose and destroyed on heating and reformed on cooling. Cooling a sol produces eventual gelatin at a temperature that seems to be reproducible. Once gelatin has occurred, the gel can be maintained at a higher temperatures up to some limit. This hysteresis permits holding the systems as either sol or gel within ranges of temperature characteristic of the material and depending also on its concentration and on the presence of other substances.

In some gels, the junction points are permanent and irreversible. Such junctions are due to chemical bonding. Such gels will come to an equilibrium volume when they are immersed in a given solvent. Of course, the junction points can move around in thermal motion. If the gels are placed in a suitable solvent, the polymer chains in the gels behave like those discussed in steric stabilization of dispersions (see Sec. 11.3) and the amount of liquid absorbed can be very large. This is swelling. The theory of swelling can be developed by calculating the chemical potential of the solvent in the gel (see Sec. 13.5; Vold and Vold, 1983).

13.2 Growth of Aggregates

Polymer gels are one example of disordered systems composed of a random agglomeration. The gel network will start to form on aggregation of molecules, particles, or polymers by diffusion. If the rate of growth is determined by diffusion, this process is called the diffusion-limited aggregation (*DLA*).

As a model of *DLA* (Fig. 13.1), Witten and Sander (1981) start with a single-seed particle at the origin of a square lattice. A second particle is added at some random site far away from the origin. It undergoes a random walk on the lattice until it reaches a site adjacent to the seed and becomes part of the growing cluster. A third particle is then introduced at a random distant point and undergoes a random walk until it also becomes incorporated into a growing cluster. The procedure is repeated until a cluster of a sufficiently large size is formed. If a particle touches the boundaries of the lattice in its random walk it is removed and another introduced. By defining $\rho(\boldsymbol{r})=1$ for the occupied site and $\rho(\boldsymbol{r})=0$ for the others, they obtained the density-density correlation function in an N-particle aggregate:

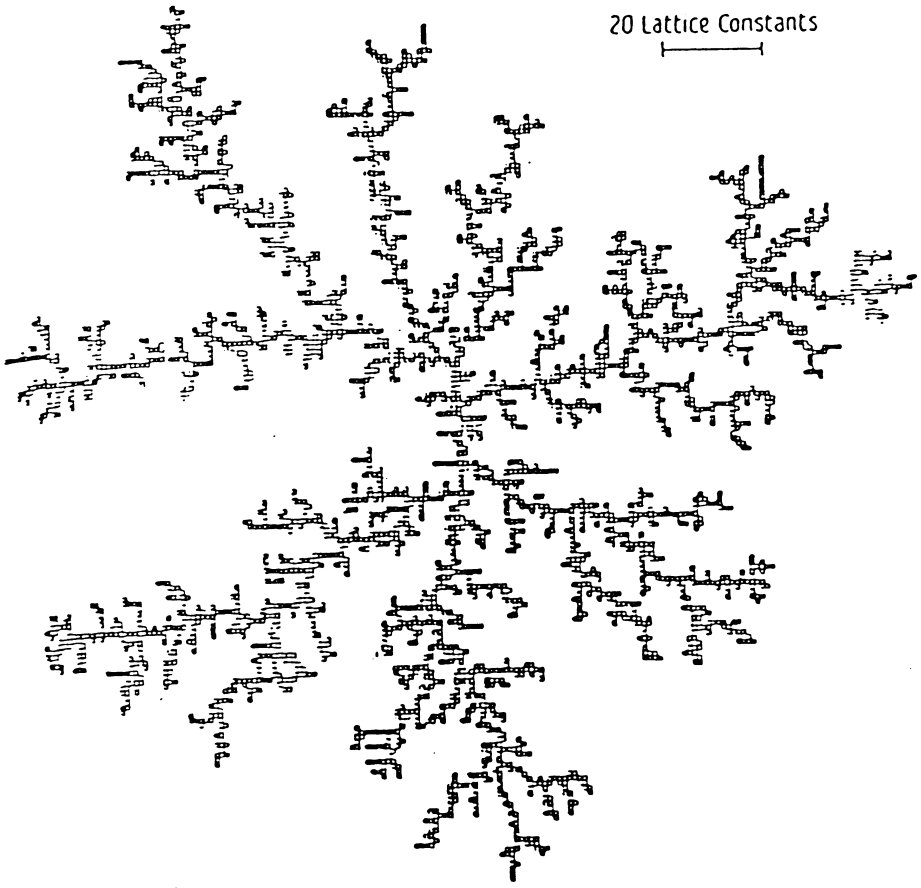

Fig. 13.1 Fractal cluster by computer simulation of DLA (WS model, the number of particles is 3600; Witten and Sander, 1981, with permission from APS).

$$C(r) = \frac{\langle \rho(\boldsymbol{r}')\rho(\boldsymbol{r}'+\boldsymbol{r})\rangle}{\langle \rho(\boldsymbol{r}')\rangle} = \frac{1}{N}\sum_{\boldsymbol{r}'} \rho(\boldsymbol{r}')\rho(\boldsymbol{r}'+\boldsymbol{r}) \sim r^{-0.343\pm0.004} \tag{13.1}$$

where $\boldsymbol{r}$ is a vector from a site to another and $r=|\boldsymbol{r}|$. The numerical exponent of Eq. 13.1 can only be true for r much less than the size of the aggregate. The average number of particles $N(a_G)$ within a neighborhood of radius of gyration a_G is then given by

$$N(a_G) = \int_0^{a_G} \mathrm{d}\boldsymbol{r}\langle \rho(\boldsymbol{r})\rangle_{\text{origin occupied}} = \int_0^{a_G} \mathrm{d}\boldsymbol{r}\langle \rho(0)\rho(\boldsymbol{r})\rangle / \langle \rho(0)\rangle$$

in the Euclidean two-dimensional space. Therefore, we have

$$N(a_{\mathrm{G}}) \propto \int_0^{a_{\mathrm{G}}} r\mathrm{d}rC(r) \sim a_{\mathrm{G}}^{2-0.343\pm0.004} = a_{\mathrm{G}}^{D}, \quad D \sim 1.68 \tag{13.2}$$

where D is the fractal dimension.

In principle, the fractal dimension does not depend on the type of the lattice but only on the Euclidean dimensionality. In fact, Witten and Sander (1981) found nearly the same exponent of Eq. 13.1 describing aggregates on a triangular lattice. Meakin (1983) numerically obtained fractal dimensions of *DLA* in Euclidean 2–6-dimensional spaces, where approximately $D \sim 5d/6$ (d: Euclidean dimension 2–6). Gouyet (1996) gave a better approximation to the fractal dimension of DLA in Euclidean space of dimensionality d:

$$D = (d^2 + 1)/(d + 1) \tag{13.3}$$

In the above *DLA* model, the permanent sticking of particles occurs once they are in contact. In another model, aggregates are formed by a diffusion-reaction process, where the permanent sticking occurs with a smaller probability ($p<1$). This model simulates the reaction-limited aggregation (*RLA*), where the rate of growth is governed by the reaction rate leading to the particle sticking. In this model a crossover occurs. Namely, after the aggregate is grown sufficiently large, the fractal dimension is independent of p and approaches to the value of the Witten-Sander model. For any value of p (<1), after N of the sites neighboring the aggregate have been visited without sticking, the probability of occurrence of the permanent sticking at an (N+1)th site in the following visit is $(1–p)^N p$. If the size of the aggregate is sufficiently small, the final sticking occurs after the particle has visited almost all of the sites neighboring the aggregate, so that it results in a dense aggregate. When the aggregate has grown large, however, the number of the neighboring sites is large and the sticking must occur in the neighborhood of the site of the first visit and thus we have approximately the *DLA* case. Therefore, the fractal dimension of a large aggregate does not depend on p, as computer simulations show in two- and three-dimensional lattices (Meakin, 1983).

As discussed in Sec. 6.3, small-angle x-ray scattering at wavelengths ranging from 1 Å to 1 μm has been used to investigate aggregates. Weitz et al. (1985) determined the fractal dimension of a gold colloid aggregate produced under conditions allowing fast, or, *DLA* as $D=1.77\pm0.05$, and that of a gold colloid aggregate under conditions of slow aggregation, or *RLA* as $D=2.05\pm0.05$.

Another model called "ballistic" stands for the case when sticking particles randomly move on directed straight lines in space like bullets (Ramanlal and Sander, 1985). If the mean free path of the particle before sticking is much smaller than the aggregate size, this model approaches the Witten-Sander model. But, if the aggregate size is much smaller than the mean free path, the fractal dimension must be 2 or 3 in the Euclidean two- or three-dimensional space, respectively. The ballistic case where particles arrive from a single direction is a model for deposition

(Family, 1990). The deposition process represents typical cases of the growth of rough surfaces (see Sec. 12.5). There are other models for deposition: random deposition and random deposition with surface diffusion. The random deposition model gives a roughest surface.

In reality, any particle can be a seed particle and many aggregates or clusters will be formed independently. Now we can expect the diffusion-limited cluster-cluster aggregation, the reaction-limited cluster-cluster aggregation, or the ballistic cluster-cluster aggregation model. The clusters usually have different sizes. For such a case, we could choose the diffusion coefficient $D_{\text{dif}}(s)$ of a cluster of size s (mass) to be

$$D_{\text{dif}}(s) = cs^{\gamma} \tag{13.4}$$

where c is a constant and $\gamma = -1/D$ for D-dimensional clusters (Exercise 13.3). Computer simulations show that average density of the aggregate formed by the cluster-cluster aggregation is less than that of the aggregate formed by the particle-cluster aggregation. $D = 2.5\sim3$ for particle-cluster and $D = 1.75\sim2.11$ for cluster-cluster in the Euclidean three-dimensional space (Dimon, et al., 1986; Gouyet, 1996, p. 131; see Exercise 13.4).

When Eq. 13.4 determines the aggregation rate, for $\gamma \gg 1$, the particle-cluster process such as *DLA* is predominant compared to the cluster-cluster process. This is because D_{dif} is large for large s and small for particles and the relative diffusion is large between particles and large aggregates, in favor for the *DLA* process to contribute the growth of the aggregate. However, the case when $\gamma < 1$ is physically more common.

The aggregation model can be refined by allowing the clusters to rotate. This does not qualitatively alter the results, but it can lead to a certain restructuring making the clusters more denser.

13.3 Sol-Gel Transition (Gelation)

There are conceptually two approaches to understand the sol-gel transition: the kinetic and percolation approach. For reviews, see Martin and Adolf (1991).

13.3.1 The Kinetic Theory

In a diffusion-limited cluster-cluster case, the aggregation dynamics may be analytically treated for a simple model of aerosols in a dilute gas, where the mean free path of particles are much larger than the size of a particle or cluster. The last condition allows to calculate the relative speed of two colliding aggregates A and B as

$$\langle v_r \rangle = \sqrt{k_B T/\mu_{AB}}\,, \quad \frac{1}{\mu_{AB}} = \frac{1}{m_A} + \frac{1}{m_B} \tag{13.5}$$

without using the assumption of the diffusion constant, Eq. 13.4, where μ_{AB} is the reduced mass. If the collision cross-section, σ_{AB}, is given by $\pi(a_A+a_B)^2$, where a_A and a_B are radii of the aggregates, A and B (assumed to be spherical), respectively, the number of collisions per unit time of aggregates B with an aggregate A is $c_B\langle v_r \rangle_{AB}$, which leads to

$$\sim c_B (k_B T)^{1/2} \left(\frac{1}{m_A} + \frac{1}{m_B}\right)^{1/2} (a_A + a_B)^2$$

where c_B is the number density of aggregate B. This can be rewritten as

$$\propto c_B (m_A^{-1} + m_B^{-1})^{1/2} (m_A^{1/3} + m_B^{1/3})^2 \tag{13.6}$$

Therefore, the total number of collisions per unit time is given by

$$c_A c_B K_{AB} \propto c_A c_B (m_A^{-1} + m_B^{-1})^{1/2} (m_A^{1/3} + m_B^{1/3})^2 \tag{13.7}$$

where K_{AB} is called the collision or reaction kernel. Wu and Friedlander (1993) gave a similar expression for the collision kernel in aerosols. Generalizing this formalism, Botet and Jullien (1984) expressed the collision kernel between an i-mer and a j-mer as follows:

$$K_{ij} \propto (i^{2\alpha} + j^{2\alpha})^{1/2} (i^{1/D} + j^{1/D})^{d-d_w} \tag{13.8}$$

where α is due to the assumption that the drift speed of the aggregate depends on the size such that $v_i \propto i^{\alpha}$ and D is the fractal dimension of the clusters. The Euclidean dimension d is that of the space and $d_w = 1$ if the motion is straight just like in the above example or 2 if it is a random walk.

In a reaction-limited cluster-cluster case, the reaction kernel will depend on the surface areas of reacting aggregates. Thus,

$$K_{ij} \propto (ij)^{\omega} \tag{13.9}$$

If the aggregates are spherical, $\omega = 1 - 1/d$. In general, if D denotes the fractal dimension, $\omega = D/d$, where $D = (d+2)/3$ (de Gennes, 1979).

We can try with the above reaction kernels in the Smoluchowski or kinetic equation for the number density of s-mers $c_s(t)$:

$$\frac{\partial c_s(t)}{\partial T} = \frac{1}{2} \sum_{i+j=s} K_{ij} c_i(t) c_j(t) - c_s(t) \sum_{j=1}^{\infty} K_{sj} c_j(t) \tag{13.10}$$

(The proportionality constant in the above kernels, Eqs. 13.8 and 13.9, is not so important to determine the general behavior of the aggregation process since it can be absorbed in t by scaling time.) In view of the physical and chemical complexity involved in the aggregation process, the above simplified models for the reaction kernels may not be necessarily appropriate. It can be more difficult to determine, reversely, the form of the kernel for a given physical system by using the above kinetic equation. In fact, this equation does not allow an analytical solution except for the following three cases (Chandrasekhar, 1943; McLeod, 1962; Ziff, 1980; also see Vicsek, 1992):

$$K_{ij} = 1\,, \quad i+j\,, \quad \text{and} \quad ij \tag{13.11}$$

Fortunately, Van Dongen and Ernst (1985) have simplified the treatment by demonstrating that the homogeneity of the kernel in the form of $i^{\mu}j^{\nu}$ dominates the time evolution of $c_s(t)$. Namely, this procedure is to determine two exponents, μ and ν, to define the type of the growth of aggregates. If $\mu>0$, large-with-large aggregation is predominant and the resultant size distribution will leave small aggregates behind. If $\mu<0$, on the other hand, small-with-large aggregation is overwhelming and the resultant size distributions are tightly bunched, like a bell-shaped curve.

For simplicity, suppose that

$$K_{ij} = ij \tag{13.12}$$

This scheme corresponds to the assumption that all sites on an aggregate are equally reactive (Stockmayer, 1943). Let us define the n-th moment of $c_s(t)$ by

$$M_n(t) = \sum_{s=1}^{\infty} s^n c_s(t) \tag{13.13}$$

From Eq. 13.10, we obtain

$$\frac{dM_n(t)}{dt} = \frac{1}{2}\sum_{i,j} c_i(t)c_j(t)K_{ij}[(i+j)^n - i^n - j^n] \tag{13.14}$$

For $n=1$, this equation shows nothing but the conservation of the total mass. For $n=2$, if $K_{ij}=ij$,

$$\frac{dM_2(t)}{dt} = [M_2(t)]^2 \tag{13.15}$$

Therefore, we have

$$M_2(t) = \frac{M_2(0)}{1 - M_2(0)t} = \frac{1}{t_c - t} \tag{13.16}$$

where $M_2(t)$ diverges at $t=t_c=1/M_2(0)$ (note that t is scaled so that it does not have the dimension of time). This implies that since the average cluster size is $M_2(t)/M_1(t)$, there appear clusters of an infinite size. This corresponds to the sol-gel phase transition (gelation) at $t=t_c$. The percolation theory gives a similar result (Eq. 13.18).

White (1980) has investigated the types of the reaction kernels K_{ij} which lead to the phase transition. For instance, he proved that the phase transition does not occur if $K_{ij} \leq i+j$. This implies that the transition is possible for *RLA* but not for DLA.

13.3.2 Percolation

We may also use the idea of percolation as a theoretical model of sol-gel transition. The word "percolation" originated from an analogy with a fluid (the water) crossing a porous medium (the coffee). Of course, the natural percolation phenomenon is much more complex than the simplified theoretical model of percolation.

Consider a resistor network. Namely, all the square lattice points (sites) bounded by four boundary edges of a large square are connected by resistors. Apply an electric potential difference across the square to the two opposite boundary edges and measure the current. We cut some of the network resistors at random. The current then flows a portion p of the resistors intact, as shown in Fig. 13.2. As more resistors are cut, the current and the value of p decrease. With $p=p_c=1/2$ (if the network is very large) it is almost certain (in the probability sense) that the current stops.

This is a model of bond percolation (resistors work as bonds among the sites) and p_c is called the bond percolation threshold.

If we remove some of the lattice sites at random, instead of cutting resistors, the percolation is called the site percolation. The threshold is $p_c=0.59$.

Figure 13.2 can also represent the conductivity of a random distribution of insulating and conducting balls. Then, $p_c \approx 0.3$.

Various percolation networks have been treated. The threshold is usually found only numerically on a finite network and then extrapolated to an infinite size. However, if a mean field approximation (Gouyet, 1996, p. 96) is used, p_c may be theoretically obtained (Essam, 1980; Stauffer, 1985). In the case of a Cayley tree (also known as a Bethe network), Fig. 13.3, where each site has z nearest neighbors, the exact solution may be found that $p_c=1/(z-1)$.

In the case of resistors (Fig. 13.2), the current is found to behave like $1/(p-p_c)^{\alpha}$ in the neighborhood of p_c. The (critical) exponent α is a number which depends on the model and the Euclidean dimension of the space. The characteristic is also found in the case of phase transitions close to the critical temperature T_c. In general, it is difficult to analytically find the value of α. A computer simulation is then a powerful method of obtaining p_c.

The motivation of introducing percolation into practice was related to oil recovery to find whether tiny pore structures in oil reservoirs are isolated or connected by a

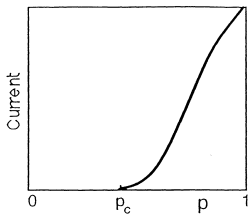

Fig. 13.2 The current as a function of p (Gouyet, 1996, with permission from Masson or Springer-Verlag).

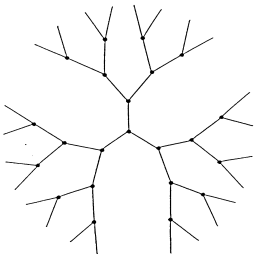

Fig. 13.3 Cayley tree with $z = 3$.

percolation phase. In the above resistor network, if the resistors are connected through sites from one boundary edge to another of the square in any possible way, it is said to be in a percolation phase and contribute to the conduction. Groups of the locally connected resistors or unconnected single resistors are, on the other hand, isolated from one another like small islands in the whole network. Such isolated groups may be considered as clusters. Below the threshold p_c, we have only the finite clusters or monomers. As the proportion p of resistors intact increases and reaches $p \geq p_c$ (= 1/2 for bond percolation in a square lattice), an infinite cluster, or percolation cluster, appears. Fig. 13.1 indicates that such clusters increase rapidly for $p \geq p_c$, showing a critical behavior at $p = p_c$. This is the sol-gel transition.

Let us consider the model in site percolation. The proportion p is then the total number of sites intact divided by the total number of used (intact) and unused (removed) sites in the whole network. In this case, the size s of a cluster is defined by the number of sites in the cluster. Therefore, if n_s is the number of clusters of size s per site, the corresponding proportion p is given by

$$p = \sum_s s n_s , \quad (p < p_c) \tag{13.17}$$

Thus, p is the first moment of Eq. 13.13. The mean number of sites in a finite cluster is defined by

$$\langle s \rangle = \sum_s s(s n_s) / \sum_s s n = \sum_s s_s / p \ .$$

If p approaches p_c from below, infinite clusters start to appear at $p = p_c$ and, according to Stauffer (1985), the mean finite cluster size is given by

$$\langle s \rangle \propto |p - p_c|^{-\gamma} \quad \text{at} \quad p = p_c \tag{13.18}$$

where

$$\gamma = 43/18 \quad \text{for} \quad d = 2$$

$$\gamma = 1.8 \quad \text{for} \quad d = 3$$

Equation 13.18 is to be compared with Eq. 13.16 of the kinetic theory.

A mean field approximation gives that $\gamma = 1$, the same exponent as given by the kinetic theory (Stauffer, 1985).

The behavior of finite clusters at the threshold is interesting in the sense of fractals in both the cluster shape and the size distribution. A cluster of size s has a certain mean radius R_s, usually defined by the radius of gyration. The value of R_s depends on the shape distribution of s-mer clusters. Numerical experiments and phase transition considerations demonstrate that the size s and R_s are both fractals at $p = p_c$ for large clusters.

$$s \propto R_s^D \quad (p = p_c) \tag{13.19}$$

where

$$D = 91/48 \quad \text{for} \quad d = 2$$

$$D = 2.52 \quad \text{for} \quad d = 3$$

It is also important that the cluster size distribution n_s is a fractal:

$$n_s \propto s^{-\nu}, \quad \text{at} \quad p = p_c \quad \text{for} \quad \text{large } s \tag{13.20}$$

where

$$\nu = 187/91 \quad \text{for} \quad d = 2$$

$$\nu = 2.2 \quad \text{for} \quad d = 3$$

It has been recognized that the percolation theory of gelation offers more information than the kinetic theory does. For instance, relations among the critical exponents of various physical quantities have been established (Gouyet, 1996).

13.4 Mechanical Properties of Gels

Many gels are truly elastic bodies in which the deformation produced by a given applied force is rapidly and completely reversible, since the network junctions remain intact throughout the process. One of the examples is rubber (Treloar, 1975). Here, the deformation is to change the configurations of polymer chains, cross-linked, from one configuration to another. The probability of occurrence of a configuration is related to the entropy.

In Sec. 11.3 we have briefly discussed the configurations of a linear polymer of n segments. If the relative arrangement of segments of a polymer obeys the statistics of (self-avoiding) random walk, the end-to-end length r of the polymer (the straight distance between the ends) satisfies approximately (see Sec. 4.1)

$$\langle r^2 \rangle = bnl^2 , \quad (b \sim 1) \tag{13.21}$$

where l is the length of a segment. The constant b depends on the way, like a valence angle, by which the segments can bend, and the magnitude of b for a paraffin-like chain is 2. We choose a coordinate system, x, y, z, in which the origin is at one end of the polymer. The position of another end has coordinates, x, y, z, so that $r^2 = x^2 + y^2 + z^2$. The probability of occurrence of r is known for random walk. Consider a function:

$$p(x, y, z) = \frac{\beta^3}{\sqrt{\pi^3}} \mathrm{e}^{-\beta^2 (x^2 + y^2 + z^2)} \tag{13.22}$$

Then, we know that this is normalized over the whole space and if we assume that $p(x,y,z)$ is the distribution function of the end point of the polymer, we can write

$$\langle r^2 \rangle = \int_{\text{whole space}} \mathrm{d}x\mathrm{d}y\mathrm{d}z \cdot r^2 p(x, y, z) = \frac{3}{2\beta^2} \tag{13.23}$$

Therefore, if we choose

$$\beta^2 = 3/(2bnl^2) \tag{13.24}$$

Equation 13.21 is satisfied. The probability function corresponds to the number of configurations for a given end point to be located within a volume element $\mathrm{d}x\mathrm{d}y\mathrm{d}z$ at r. Since the entropy is proportional to the logarithm of the probability, for an isolated polymer the entropy is given by

$$s = c - k_\mathrm{B} \beta^2 r^2 \tag{13.25}$$

The constant c indicates that $p(x,y,z)$ is a relative probability, not absolute. The constant c is associated with the probability of choosing the chains and arranging them for cross-linking in the solvent and it depends on the volume and temperature.

As experimentally observed to a good approximation, it is usually assumed in discussing the elasticity of rubber that the internal energy does not change under deformation of rubber at constant temperature. Therefore, $\mathrm{d}U=\mathrm{d}W+T\mathrm{d}S=0$ for a polymer chain of rubber, where $\mathrm{d}W$ is work done on the chain. The tension (tensile force) on a chain under stretching at constant temperature therefore is given by

$$\mathrm{d}W/\mathrm{d}r = -T\mathrm{d}s/\mathrm{d}r = 2k_{\mathrm{B}}T\beta^2 r \tag{13.26}$$

Since the tension is proportional to the end-to-end length, the molecule obeys Hooke's law, like a classical spring. But, note that the tension, Eq. 13.26, is the average value over a period of time, since it thermally fluctuates even if the end points of the chain are fixed. In addition, we must note that the Gaussian approximation used above limits the use of Eq. 13.26. Namely, the distance r should not be more than about one-third of the contour length (the fully-extended length) of the chain.

Suppose that the polymer is deformed, so that the new position of the end has coordinates:

$$x' = \alpha_1 x\,, \quad y' = \alpha_2 y\,, \quad z' = \alpha_3 z \tag{13.27}$$

the other end being at the origin. The quantities, α_1, α_2, α_3, are called the extension ratios. Suppose that such polymers make a network of rubber. Since rubber exhibits no volume change in the deformation to a good approximation, we have

$$\alpha_1\alpha_2\alpha_3 = 1 \tag{13.28}$$

If the tensile strains are denoted by ε_1, ε_2, and ε_3, respectively, we have

$$\alpha_i = 1 + \varepsilon_i\,, \quad (i = 1,2,3) \tag{13.29}$$

(The strains can be large in rubber.) Using Eq. 13.25, the entropy change is given by

$$\Delta s = s' - s = -k_{\mathrm{B}}\beta^2[(\alpha_1^2 - 1)x^2 + (\alpha_2^2 - 1)y^2 + (\alpha_3^2 - 1)z^2] \tag{13.30}$$

Now let us consider N similar chains with n segments each. The total entropy change in a deformation is given by

$$\Delta S = \sum_{i=1}^{N} \Delta s_i$$
$$= -k_B\beta^2 \left[(\alpha_1^2 - 1) \sum_i x_i^2 + (\alpha_2^2 - 1) \sum_i y_i^2 + (\alpha_3^2 - 1) \sum_i z_i^2 \right]$$

Since $\sum x_i^2$, $\sum y_i^2$, and $\sum_i^2$ are for the undeformed state of the network, they are isotropic and each of them is equal to $(1/3)\sum r_i^2$. From Eqs. 13.21 and 13.24, if $b=1$,

$$\sum r_i^2 = N\langle r^2 \rangle = Nnl^2 = 3N/(2\beta^2)$$

Therefore, we have

$$\Delta S = -\frac{1}{2} k_B N(\alpha_1^2 + \alpha_2^2 + \alpha_3^2 - 3) \tag{13.31}$$

Note that this does not depend on the number of segments in a chain, as long as the chain coordinates, (x, y, z), distribute according to Eq. 13.22.

The number N of polymers can now be considered to be the total number of chains, irrespective of the contour length or n, in a network and ΔS is the entropy change of the rubber. In the network, the normal cross-linking (in which four chains meet at each junction point) N is simply twice the number of cross-links. We assume that the network arrangement of the chains does not change in the deformation, even though the junctions can undergo micro-Brownian motion. In addition, the unstrained state is represented by Eq. 13.21. Flory (1944) considered network defaults as deviations from the ideal case of cross-linking. If the network defects exist in the network, the number of chains participating to rubber elasticity will be accordingly reduced from the total number. Then, we need to correct the value of N.

The behavior of the network in a good or poor solvent is similar to that for the steric behavior in dispersions (see Sec. 11.3), leading to swelling or shrinking of gels (see Sec. 13.5).

The internal energy does not change during a reversible deformation of rubber at constant temperature. If we denote by W the work done by the deformation, we have $W=-T\mathrm{d}S$, where $\mathrm{d}S$ is the entropy change accompanying the deformation. Thus, Eq. 13.31 can be rewritten as

$$W = \frac{1}{2} k_B TN(\boldsymbol{\alpha}^2 - 3) \tag{13.32}$$

where $\boldsymbol{\alpha}=(\alpha_1, \alpha_2, \alpha_3)$. W is the stored energy in the deformation. For simplicity, we write

$$G = k_B TN/V \tag{13.33}$$

where V is the volume of the network system.

Simple elongation in the x direction at a constant volume is defined by, for instance,

$$\alpha_1 = a \quad \text{and} \quad \alpha_2 = \alpha_3 = a^{-1/2} \quad (\alpha_1\alpha_2\alpha_3 = 1) \tag{13.34}$$

Using Eq. 13.32, we obtain the work done per unit volume:

$$W = \frac{1}{2}G(a^2 + 2/a - 3)$$

If this elongation is carried out under an atmosphere and if the volume changes, the work done by the atmospheric pressure must be included. But, in the present case, it is small. Suppose that the elongation by $d\varepsilon$ takes place under a tensile force f at constant temperature. If W refers to a unit cube in an unstressed state, f is the force per unit area in an unstressed state. Then, the work done is $dW = f d\varepsilon$ (f and $d\varepsilon$ are the same direction). Therefore,

$$f = (dW/d\varepsilon)_T = G(a - a^{-2})(da/d\varepsilon)_T \tag{13.35}$$

Since the elongation is in the x direction, the stress τ, the force per unit area in a stressed state is related to f by

$$f = \tau\alpha_2\alpha_3 = \tau/a \quad \text{or} \quad \tau = f\alpha_1 = fa$$

Thus, f and τ have different values and we have to distinguish them for large strain. Using Eq. 13.35, for small strain we have, noting that $a = 1+\varepsilon$,

$$f = 3G\varepsilon \tag{13.36}$$

Simple shear is a type of strain which may be represented by the sliding, say, in the x direction of planes parallel to a given, say, x-z plane. It is by definition a constant-volume deformation. The three principal extension ratios may then be written as

$$\alpha_1 = a\,, \quad \alpha_2 = 1/a\,, \quad \text{and} \quad \alpha_3 = 1 \quad (\alpha_1\alpha_2\alpha_3 = 1) \tag{13.37}$$

The shear σ is defined by $\alpha_1 - \alpha_2 = a - 1/a$ (Love, 1944). Therefore, the shear stress is given by

$$\tau_{xy} = dW/d\sigma = G\sigma \tag{13.38}$$

Geometrically, note that simple shear involves a rotation added to pure shear.

Usually, the elastic deformation of a gel is accompanied by a volume change. In this case, Eq. 13.31 must be replaced by

$$\Delta S = -\frac{1}{2}k_{\mathrm{B}}N[\boldsymbol{\alpha}^2 - 3 - \ln(\alpha_1\alpha_2\alpha_3)] \tag{13.39}$$

Here, N is the effective number of polymers per unit volume.

Tanaka et al. (1973) used light scattering to measure the shear and elastic moduli of aqueous 5% and 2.5% polyacrylamide gels. Thermal fluctuations in shape of small volume elements within the macroscopically undeformed gel exhibit frequency shifts of scattered light. Ultrasonic waves were introduced to observe the relaxation, which may be due to friction between network and liquid. They obtained the value of the elastic moduli which are proportional to the number of effective polymers (Eqs. 13.33 and 13.39) and hence the number of cross-links. The amounts of the gelator were 5% and 2.5% in the samples, but the observed values of the effective numbers differed by a factor of 10^2.

13.5 Chemical Potential of Solvent in Gels

Let us consider a gel in a solvent. In Sec. 11.3 we have discussed that if a solvent has a strong interaction with a polymer (a good solvent), the polymer in the solvent spontaneously stretch itself to be well surrounded by solvent molecules. The gel will behave in a similar way in a good solvent, leading to swelling of the gel. If N_1' polymers form a gel network and N_3' solvent molecules flow into the gel, the gel will expand to a new volume, $V = V_0 + N_3' v_3$, where V_0 is the volume of the polymer network itself and v_3 is the volume of the solvent molecule (the molar volume divided by the Avogadro number). Then, the volume expansion ratio is $V/V_0 = 1 + N_3' v_3/V_0$. The gel now consists of a mixture of N_1' polymers and N_3' solvent molecules. In order to determine the chemical potential of the solvent in the gel we need the change of the Gibbs free energy involved in the swelling process.

Following the discussion of Sec. 11.3, we consider interaction energies among polymers and solvent molecules. They are denoted by W_{11} for polymer segment-segment, by W_{33} for solvent-solvent, and by W_{13} for polymer segment-solvent interactions, where the word "solvent" implies the solvent molecule. When they are mixed, the change in the interaction energies is given by Eq. 11.23:

$$\Delta W = W_{13} - (W_{11} + W_{33})/2 \tag{13.40}$$

Now we consider the change in the enthalpy per unit volume due to mixing N_1' polymers and N_3' solvent molecules. We must total the interactions of all chain segments and all solvent molecules of the gel. As in Sec. 11.3, define $N' = nN_1' + N_3'$, where n is the number of segment per polymer, and z by the

nearest neighbors of segments or solvent molecules in solution. Note that N of Eq. 13.39 is N_1' here. Then we have (Eq. 11.12)

$$\Delta H_{\mathrm{M}} = zN\varphi_1\varphi_3\Delta W = znN_1'\varphi_3\Delta W = zN_3'\varphi_1\Delta W \tag{13.41}$$

where $\varphi_1 = nN_1'/N'$ and $\varphi_3 = N_3'/N'$, volume fractions (the volume of the polymer segment was assumed to be the same as the volume of the solvent molecule in the lattice model described in Sec. 11.3). In the model, $v_3 = v_1$ (segment volume), $\varphi_1 = nN_1' v_1/(nN_1' v_1 + N_3 v_3) = V_0/V$.

In addition, we have a change of the entropy due to mixing.

$$\Delta S_{\mathrm{M}} = -k_{\mathrm{B}}[N_1' \ln \varphi_1 + N_3' \ln \varphi_3] \tag{13.42}$$

For a constant temperature process, $\Delta G = \Delta H - T\Delta S$, which can be obtained by using Eqs. 13.39, 13.41, and 13.42. Note that Eq. 13.39 is per unit volume, while we consider here only one gel network containing N_1' polymers. By differentiating ΔG with respect to N_3', we find the change in the chemical potential of solvent in the gel. But, before doing this, we first note that swelling of the polymer network is isotropic, so that $\alpha_1 = \alpha_2 = \alpha_3 \equiv \alpha$. By definition, $\alpha_1\alpha_2\alpha_3 = \alpha^3 = V/V_0 = 1 + N_3' v_3/V_0 = 1/\varphi_1$. Therefore, we have

$$\begin{aligned} \mathrm{d}\alpha^3/\mathrm{d}N_3' &= (\mathrm{d}/\mathrm{d}N_3')(1 + N_3' v_3/V_0) = v_3/V_0 = 3\alpha^2(\mathrm{d}\alpha/\mathrm{d}N_3') \\ \mathrm{d}\alpha/\mathrm{d}N_3' &= v_3\varphi_1^{2/3}/(3V_0) \end{aligned} \tag{13.43}$$

In addition, since nN_1' is constant and $\varphi_1 + \varphi_3 = 1$ during the process of mixing,

$$\mathrm{d}\varphi_1/\mathrm{d}N_3' = -\mathrm{d}\varphi_3/\mathrm{d}N_3' = -\varphi_1/N' \tag{13.44}$$

Therefore, after all, the chemical potential of the solvent in the gel is given by $\mathrm{d}\Delta G/\mathrm{d}N_3'$ or

$$\mu_3 - \mu_3^0 = k_{\mathrm{B}}T\left[\ln(1-\varphi_1) + \varphi_1 + \frac{z\Delta W}{k_{\mathrm{B}}T}\varphi_1^2 + \frac{v_3 N_1'}{V_0}\left(\varphi_1^{1/3} - \frac{\varphi_1}{2}\right)\right] \tag{13.45}$$

Here φ_1 is the volume fraction of polymers in the gel network. Since N_1'/V_0 is the effective number of polymers per unit volume, we can replace it by N of Eq. 13.39.

In the isothermal process at constant pressure, Eq. 13.45 must vanish. This condition determines the equilibrium value of the volume expansion $V/V_0 = 1/\varphi_1$. This corresponds to the maximum swelling ratio. Since $\varphi_1 \ll 1$, $\varphi_1^{1/3} \gg \varphi_1$ and approximately

$$\left(\frac{V_{\max}}{V_0}\right)^{5/3} = \frac{1}{Nv_3}\left(\frac{1}{2} - \frac{z\Delta W}{k_B T}\right) \tag{13.46}$$

Experimentally, the values of ΔW can be determined by observing V/V_0, if the effective number density of polymers is known. Gee (1946) obtained the results with vulcanized natural rubber in various solvent and showed that they were reasonably well compared with values from vapor pressure studies.

When φ is large (closer to unity), $z\Delta W/k_B T$ is known to depend on the concentration of polymers, φ_1. Expanding we write

$$z\Delta W/k_B T = \chi_1 + \chi_2\varphi_1 + \chi_3\varphi_1^2 + \cdots \tag{13.47}$$

Hökev et al. (1971) experimentally observed this dependence with a system of polystyrene in cyclohexane and showed that it behaved like a poor solvent at larger concentration of polystyrene. This is a reasonable result since the segment-solvent interaction will be effectively weak if the amount of the solvent is not large enough to cover all the polymers of the gel.

In Sec. 11.3, it is discussed that, if polymer segments are covalently bonded to neighboring segments, Eq. 8.8 cannot be used to write $W_{13}=(W_{11}W_{33})^{1/2}$. But, if the bonding covalence is relatively weak, we may approximately write

$$\Delta W = (W_{11}^{1/2} - W_{33}^{1/2})^2$$

If we use the lattice model (Sec. 11.3), where $v_1 = v_3 = v$, the total volume of the gel is $V=(nN_1'+N_3')\,v$. Equation 13.41 may then be rewritten as

$$\Delta H_M = zV\varphi_1\varphi_3[(W_{11}/v_1)^{1/2} - (W_{33}/v_3)^{1/2}]^2 \tag{13.48}$$

$$\equiv zV\varphi_1\varphi_3(\delta_1 - \delta_3)^2\,, \quad \delta_i \equiv (W_{ii}/v_i)^{1/2} \tag{13.49}$$

where δ_i is the square root of the cohesive energy density of either polymers or solvent molecules. The values are listed by Burnell (1975) and they range from 5 to 14 $(\text{cal cm}^{-3})^{1/2}$. For water it is particularly large with the value of 23.4 $(\text{cal cm}^{-3})^{1/2}$. The quantity δ_i is closely related to Hildebrand's solubility parameter. If we know the values, Eq. 13.48 may be used for estimating the enthalpy of mixing.

The charge on ionic network produces a very high degree of swelling when the gel is immersed in pure water. However, solutions of electrolyte reduce the swelling markedly.

The elastic moduli of a gel depend on the degree of swelling. If the swelling is represented by φ_1 (possibly, $V_{\max}/V_0$ of Eq. 13.46), G of Eq. 13.33 must be replaced by

$$G = k_B T N \varphi_1^{1/3} \tag{13.50}$$

where N is per unit volume.

13.6 Rheological Properties of Gels

In Sec. 4.4, rheological properties of disperse fluids are discussed and the Voigt model is considered as a suitable method for studying elastic properties of gels. However, it is usually not easy to observe the instantaneous initial deformation of gels right after an external force is exerted. In order to analyze the rheological behavior in this case, therefore, a compound model of the Voigt model and a dashpot in series may be used. An example is an experiment on a living egg of a sea-urchin. Hiramoto (1969) immersed a tiny iron sphere in the egg and observed its temporal displacement under a magnetic field (a constant force of $3.6 \cdot 10^{-4}$ dynes). It moved as far as a distance of about 20 μm after one second. The magnetic field was then removed, but the sphere did not return to its initial position, leaving a permanent deformation ($\sim$10–15 μm) in the egg. He placed the iron sphere at three different places in the egg, but the behavior did not depend on the positions. He observed, however, differences in the rheological behavior among not-well-grown, fully grown, and fertilized eggs.

The dynamical models (see Sec. 4.4) are convenient to systematically organize dynamical data of gels, but it hardly clarify detailed molecular structure of gels. Recently, much research has been conducted on gels at the molecular level by using neutron magnetic resonance (NMR) experiments. Large molecules are intrinsically mobile, and the knowledge of internal motions is necessary for an accurate description of three-dimensional structures and an understanding of their chemical reactivity. NMR spectroscopy is capable of providing information on molecular dynamics, including rotational and translational diffusion, segmental motions, restricted and self-diffusion, conformational equilibria, inter- and intramolecular rate processes. For details see Delpuech (1995).

13.7 Applications of Gels

There are wide applications of gel states. If gels are swollen in water, they are called hydrogels. If the solvent is an organic material, they are called organogels. Many gels with which we are familiar, such as gelatin, vegetation, highly hygroscopic synthetic polymer gels, etc., are hydrogels. Organogels are not so popular, but they have started to appear. For instance, gels, which are treated in silicon oil

as a solvent, are used as a shock absorber. If the solvent is alcohol, they are called alcogels. If it is ethyl alcohol, the alcogels may be used for chickens as a sedative to avoid troubles originating stress among them.

Biological systems are mainly made of gels. Hydrogels are closest to the biological gels in the sense of controlling surrounding to a constant condition. Medical applications of hydrogels include, therefore, material for cultivating bacteria, soft contact lenses, artificial skin, artificial joint, food technology, cosmetics, etc.

It is necessary to maintain agricultural soil in a gel state in order to achieve good aeration and drainage. Highly hygroscopic hydrogels can also be used, for this purpose, in mixture with soil to keep moisture around. However, polymers of hydrogels could be dissociated by microorganism or various ions in soil and lose the ability of aeration and drainage.

Highly hygroscopic polymers can gelatinize liquid. This capability can be used to convert a liquid medicine to a gel, which can be easily fed to chickens.

In oil-well drilling, removing the cuttings and sealing the bore wall are made effective if a drilling mud (a bentonite clay suspension) is converted to a gel by a peptizing agent, such as a polyphosphate. A paint should be designed to brush easily and yet flow on a vertical surface; this is achieved by making the paint thixotropic.

Gels are also used to make construction materials, such as water sealing material, artificial snow, hydrogels mixed with cement to increase strength, etc. Silicon gels (polymers, carbon atoms of which are replaced by silicon atoms, bridge in the gel network) have excellent properties as electrical insulating material, which can be used as a hybrid IC module for automobile engine electronics, a power module for machinery, etc. Electro-rheological fluid has usually a good fluidity but loses it under an electric field. It can be used, therefore, as a fluid damper, clutch, and actuator.

Some gels behave like ultrafilter membranes of very large pore of 100 Å or as large as 8000 Å (cellulose membranes). One application is gel permeation chromatography, which is of great value in biochemical and medical research. Ion exchange resins are widely used.

Exercises

13.1 Why is the rotational relaxation time of water molecules near the gel framework so high?

13.2 In the random deposition model, the particles fall vertically at random onto a horizontal surface and pile up vertically. The height at each pile has no correlation. Then, what is the standard deviation of the height distribution?

13.3 Show that Eq. 13.4 leads to the form of Stokes' law for a spherical particle. (General discussion in de Gennes (1979).)

13.4 How is the fractal dimension related to the mean density of a cluster? (The dimension is larger for the aggregates formed by a particle-cluster aggregation process,

since particles can penetrate into a cluster before sticking compared to penetration of clusters into a cluster.)

13.5 Suppose that $K_{ij}=i^{\mu}j^{\nu}$. Discuss the aggregation process as to a large-large or small-large aggregation if $i \ll j$ and $\mu>0$. Which process, large-large or small-large, is predominant?

13.6 Establish Eq. 13.15 and solve it to obtain Eq. 13.16.

13.7 In Eq. 13.19, imagine the possible shapes of finite cluster s for $d=3$.

13.8 A gel undergoes an elastic deformation isothermally. Show that the work done is equal to the change of Helmholtz free energy ($\mathrm{d}W=\mathrm{d}F$ at constant temperature).

13.9 Consider rubber, which consists of a polymer network and does not change the volume under stretching. Show then that, if the stretching is carried out adiabatically, the temperature rises.

13.10 Noting that the internal energy of rubber and the volume do not change under a mechanical deformation under constant temperature, show that Eq. 13.32 with Eq. 13.33 leads to

$$\tau_1 - \tau_3 = G(\alpha_1^2 - \alpha_3^2) \quad \text{and} \quad \tau_2 - \tau_3 = G(\alpha_2^2 - \alpha_3^2)$$

where τ_1, τ_2, and τ_3 are the principal stresses in the strained state. A simple elongation in the x direction at constant temperature, τ_2 and τ_3 vanish and the above relations result in Eq. 13.35.

13.11 Establish Eq. 13.38.

13.12 Discuss the behavior of the network of charged polymers in pure water and aqueous electrolyte solutions.

13.13 Establish Eq. 13.45.

13.14 Derive Eq. 13.46.

13.15 Derive Eq. 13.48.

13.16 Verify Eq. 13.50.

References

Alexander, A.E. and Johnson, P., "Colloid Science", Oxford Univ. Press (Clarendon), London (1949), p. 602.

Botet, R. and Jullien, R., *J. Phys. A 17*, 2517 (1984).

Brown, W. and Chitumbo, K., *J. Chem. Soc. Faraday Trans. I 71*, 1 (1975).

Burnell, H. in "Polymer Handbook", 2nd ed., eds., Brandrup, J. and Immergut, E.H., Wiley, New York (1975).

Chandrasekhar, S., *Rev. Mod. Phys. 15*, 1 (1943).

de Gennes, P.G., "Scaling Concepts in Polymer Physics", Cornell Univ. Press, Ithaca, New York (1979).

Delpuech, J.-J., ed., "Dynamics of Solutions and Fluid Mixtures by NMR", John Wiley & Sons, New York (1995).

Dimon, P., Sinha, S.K., Weitz, D.A., Safinya, C.R., Smith, G.S., Varady, W.A., and Lindsay, H.M., *Phys. Rev. Lett. 57*, 595 (1986).

Essam, J.W., *Rep. Prog. Phys. 43*, 833 (1980).

Family, F., *Physica A 168*, 561 (1990).

Flory, P.J., *Chem. Rev. 35*, 51 (1944).

Gee, G., *Trans. Faraday Soc. 42B*, 33 (1946).
Gouyet, J.F., "Physics and Fractal Structures", Masson, Springer-Verlag, Paris, Berlin (1996).
Higuchi, A. and Iijima, T., *Polymer 26*, 1207 (1985).
Hiramoto, Y., *Experimental Cell Research 56*, 201 (1969).
Hökev, H., Shih, H., and Erman, B., *Trans. Faraday Soc. 67*, 2275 (1971).
Love, A.E.H. "A Treatise on The Mathematical Theory of Elasticity", Dover Publications Inc., New York (1944).
Martin, J.E. and Adolf, D., *Annu. Rev. Phys. Chem. 42*, 311 (1991).
McLeod, J.B., *Quart. J. Math. Oxford 13*, 119 (1962).
Meakin, P., *Phys. Rev. A 27*, 1495 (1983).
Ramanlal, P. and Sander, L.M., *Phys. Rev. Lett. 54*, 1828 (1985).
Stauffer, D., "Introduction to Percolation Theory", Taylor and Francis, London (1985).
Stockmayer, W.H., *J. Chem. Phys. 11*, 45 (1943).
Tanaka, T., Hocker, L.O., and Benedek, G.B., *J. Chem. Phys. 59*, 5151 (1973).
Tokita, M., Terakawa, K., Ikeda, T., and Hikichi, K., *Polymer Communications 31*, 38 (1990).
Treloar, L.R.G., "The Physics of Rubber Elasticity", Oxford Univ. Press (Clarendon), London (1975).
Van Dongen, P.G. and Ernst, M.H., *Phys. Rev. Lett. 54*, 1396 (1985).
Vicsek, T., "Fractal Growth Phenomena", 2nd ed., World Scientific Publ., Singapore (1992).
Vold, R.D. and Vold, M.J., "Colloid and Interface Chemistry", Addison-Wesley, Reading, MA (1983).
Weitz, D.A., Huang, J.S., Lin, M.Y., and Sung, J., *Phys. Rev. Lett. 54*, 1416 (1985).
White, W.H., *Proc. Am. Math. Soc. 35*, 273 (1980).
Witten, T.A.,Jr. and Sander, L.M., *Phys. Rev. Lett. 47*, 1400 (1981).
Wu, M.K. and Friedlander, S.K., *J. Aerosol Sci. 24*, 273 (1993).
Ziff, R.M., *J. Stat. Phys. 23*, 241 (1980).